Progress In Electromagnetics Research M, Vol. 115, 45–58, 2023

A Miniaturized Ultra-Wideband MIMO Antenna Design with Dual-Band Notched Characteristics

Xuan Lu[1, *], Shushu Linghu[1], Furong Peng[2], and Ting Zhang[1]

Abstract—In this manuscript, a miniaturized Multi-Input Multi-Output (MIMO) antenna with dual-notch characteristics is designed for Ultra-Wideband (UWB) indoor positioning system. The proposed UWB MIMO antenna has a compact size of $35 \times 35\,\text{mm}^2$ with four orthogonally placed antenna elements on the print circuit board (PCB) with FR4. Each radiating element utilizes the combination of a rectangle and an irregular pentagon, and etches two inverted L-shaped slits to generate two notches in WLAN (5.00 GHz–5.82 GHz) and X-band (7.11 GHz–8.20 GHz). On the grounding planes, the rectangle grounding units are modified into L-shaped branches, on which stepped open-circuit slots and right-angled triangle truncations are etched to broaden the impedance bandwidth. Furthermore, three equidistant rectangular decoupling slits are etched to improve the isolation. The measured results are in good agreement with the simulated ones, which shows an impedance bandwidth of 116.68% (2.96–11.25 GHz) with isolation better than 17 dB. The antenna also has excellent characteristics of good radiation characteristics, total active reflection coefficient (TARC), diversity gain (DG $>$ 9.99), low envelope correlation coefficient (ECC $<$ 0.005), and channel capacity loss (CCL $<$ 0.4 bits/sec/Hz), which can be used in portable UWB-MIMO indoor positioning system.

1. INTRODUCTION

Indoor positioning based on UWB technique has the advantages of strong stability, strong anti-interference ability, and high positioning accuracy, and has been widely used in the field of location services [1]. The Federal Communications Commission (FCC) has allocated the 3.10–10.60 GHz frequency band for UWB commercial applications. However, this band is of co-occurrence with WiMAX (3.3–3.7 GHz), wireless local area network (WLAN, 5.15–5.825 GHz), and X-band satellite (7.25–7.75 GHz). Thus, it is necessary to design UWB antennas with notch band characteristics to alleviate the interference of these narrow band communication systems [2]. Currently, different frequency notch techniques are designed and etched on the radiation patch, feeder, or ground plane to realize band notch characteristics, including slots of different shapes, narrow-band resonance branches, and parasitic resonance structures [3–16].

MIMO antennas are used at the transmitter and receiver terminals to enhance data transmission capacity and reduce multipath fading [17]. In application of the compact UWB indoor positioning system, miniaturization of the MIMO antenna is an important factor to consider. However, miniaturization is paradoxical to high isolation among MIMO antenna elements, which increases the difficulties of band notch and decoupling. In the past few years, some commonly used decoupling techniques include diversity methods, defected ground structure (DGS), adding parasitic branches, neutralizing line methods, loading electromagnetic band-gap (EBG) structure, etc. In [17], a T-shaped slot was etched on the ground plane to reduce the mutual coupling effect, and the mutual coupling

Received 16 November 2022, Accepted 18 January 2023, Scheduled 30 January 2023
* Corresponding author: Xuan Lu (xuanlu@sxu.edu.cn).
[1] College of Physics and Electronic Engineering, Shanxi University, Taiyuan 030006, China. [2] Institute of Big Data Science and Industry, Shanxi University, Taiyuan 030006, China.

value can be suppressed up to a level of −16 dB in the band of operation. Another method of inserting neutralization lines between radiation patches was proposed in [18]. The authors of [19] used four identical elliptical shaped monopole radiators located orthogonally to each other. And the second order Koch fractal geometry was used at the edge of the ground plane to extend the impedance bandwidth. For reducing inter-element coupling in the proposed MIMO antenna, a different approach (of slotted edge substrate) was used, as a substitute of traditional decoupling stub/elements. In [20], a compact quad-element MIMO antenna was proposed, which is suitable for a wide range of UWB applications. The proposed antenna used a hexagonal molecular-fractal structure as the radiation element. In order to yield good isolation, the antenna elements were placed orthogonally to each other. The mutual coupling value in the operating band can be suppressed up to a level of −20 dB. In [21], the authors achieved a simple but effective four port UWB MIMO antenna. The phenomenon of the polarization diversity by deploying four orthogonal antenna elements was used to enhance the isolation between the MIMO antenna elements. The antenna elements were reduced in size by modifying the patch shape and placing them close to each other to reduce unnecessary interaction between the antenna elements. In [22], a novel MIMO UWB antenna with dual notches was proposed. The antenna used a Quasi Self Complementary (QSC) method to extend the bandwidth. The dual notched bands (WiMAX at 3.6 GHz and the WLAN band at 5.8 GHz) were achieved by using a square ring printed on the bottom of the substrate and etching a C-shaped slot in the radiating patch. In the proposed MIMO antenna, the isolation reduction was achieved utilizing diversity technique to minimize the mutual coupling between the antennas.

The purpose of this paper is to achieve high isolation and double notch band characteristics on the premise of the miniaturization of four-element UWB MIMO antennas. The elements are identical and orthogonally placed on both sides of the substrate. Each element is composed of an irregular pentagonal patch and an elaborate ground. Two notched bands are realized by etching two inverted L-shaped slits on the patch, and a decoupling structure of three equidistant rectangular slits is etched on the ground as well. The structure of the design is presented in detail in the following sections.

2. ANTENNA STRUCTURE DESIGN

2.1. Antenna Structure

The structure of the UWB MIMO antenna with dual-band notched characteristics is shown in Figure 1. The antenna is printed on a low-cost 1.6 mm-thick FR4 substrate, with a total size of $35 \times 35\,\text{mm}^2$, a relative permittivity of 4.4, and a loss tangent of 0.02. The specific dimensions of the simulated optimized geometric parameters are shown in Table 1.

Table 1. Parameters of the proposed antenna.

Parameters	W	L	$W1$	$L1$	$W2$	$L2$	$W3$	$L3$	$W4$	$L4$	$W5$
Value (mm)	35	35	6	8	5	0.5	12	7	1.5	2.5	2.4
Parameters	$L5$	$W6$	$L6$	$L7$	$W8$	$L8$	m	g	t	$t1$	$t2$
Value (mm)	1	6.4	3.5	20.5	6.5	3.6	15.9	2	1.3	0.4	0.5
Parameters	$t3$	$X1$	$X2$	$Y1$	$Y2$	Lp					
Value (mm)	0.2	3.7	5.4	2.6	3.2	0.4					

The design steps of the antenna are shown in Figures 2(a)–(d). Initially, a basic MIMO antenna is composed of four orthogonally placed monopole UWB elements shown in Figure 2(a). Each element has an irregular pentagon patch fed by a microstrip line and a rectangular ground plane. To broaden the bandwidth, the rectangular grounds are elaborately modified in Figure 2(b), on which stepped open-circuit slots and right-angled triangle truncations are etched as well. In Figure 2(c), two inverted L-shaped slits are etched on each radiation patch, achieving dual-band notched rejections in WLAN (5.00 GHz–5.82 GHz) and X-band (7.11 GHz–8.20 GHz). Finally in Figure 2(d), three equidistant

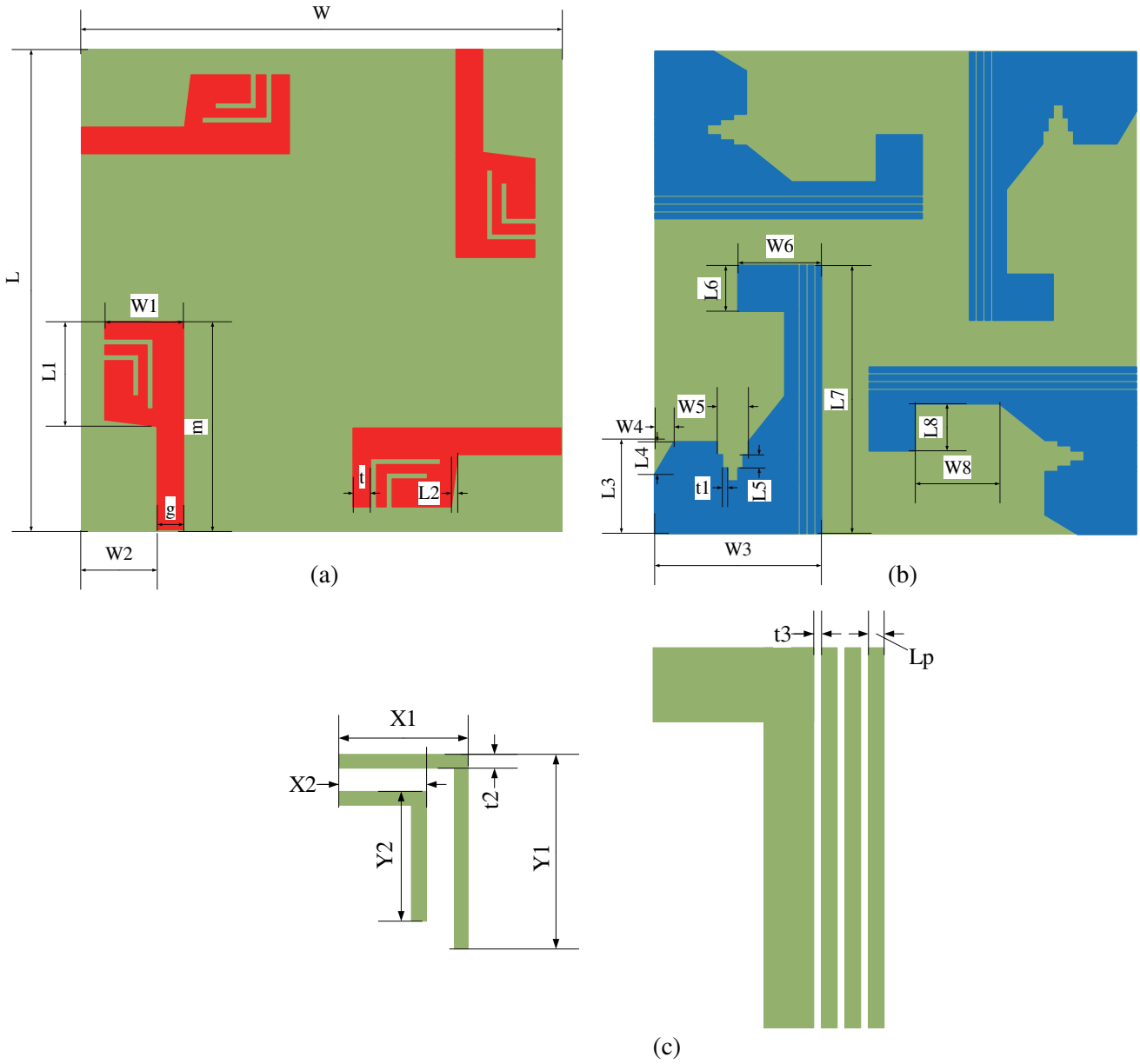

Figure 1. Geometry of proposed compact four element UWB MIMO antenna: (a) top view; (b) bottom view (unit: mm); (c) local detail size.

rectangular slits are etched on each ground plane element to form decoupling slits, which can especially reduce mutual coupling at low frequencies.

The antenna performances of the four steps are compared in Figure 3. It can be seen that the lower cut-off frequency of $S_{11} < -10$ dB becomes 2.88 GHz from 6.06 GHz due to the modification of the ground, realizing a bandwidth of 2.88 GHz–10.60 GHz as shown in Figure 3(a). After etching two inverted L-shaped slits on radiation patches, two notches of $S_{11} > -10$ dB are obtained at 5.00 GHz–5.82 GHz and 7.11 GHz–8.20 GHz. At 5.20 GHz and 7.80 GHz, S_{11} reach -3.92 dB and -4.97 dB, respectively. Besides, the S_{11} curve is almost unchanged by introducing decoupling slits. The isolation performance is illustrated in Figures 3(b)–(d). It can be seen that S_{21}, S_{31}, and S_{41} of each port are reduced to less than -17 dB at the entire operating band by the decoupling slits, and S_{21} and S_{41} are almost identical because of the symmetrical structure.

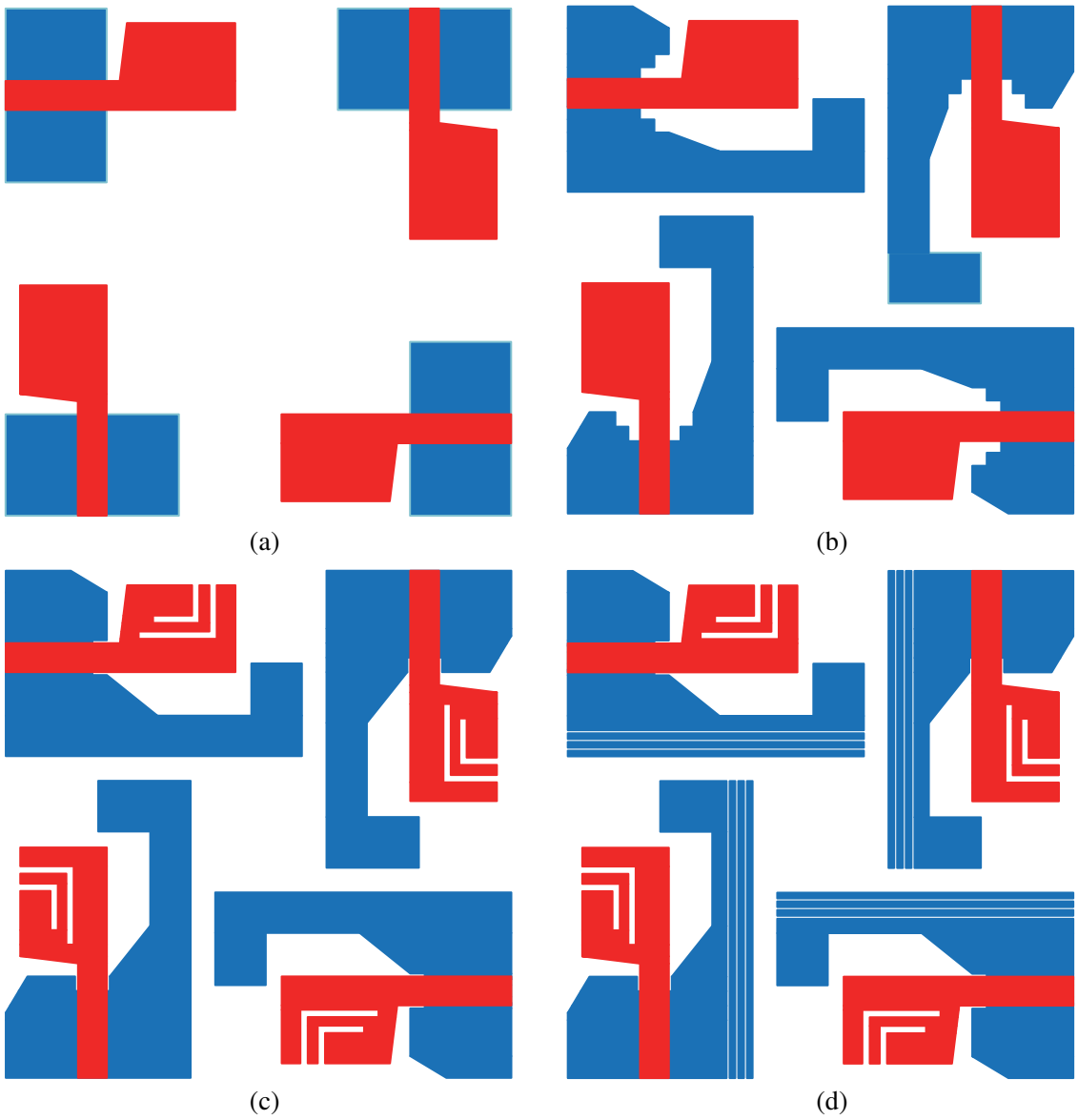

Figure 2. Design steps of the antenna: (a) a basic MIMO antenna with four monopole UWB elements (rectangular ground plane); (b) the ground plane is modified to broaden the bandwidth; (c) dual-band notch characteristics are realized by etching two inverted L-shaped slits; (d) three equidistant decoupling slits are added in the ground plane for a final design.

2.2. Notch Principle

The dual-band notched characteristics are realized by etching two inverted L-shaped slits of $\lambda/4$ on the radiation patch. The total length l_t of each slit is obtained by Equations (1), (2), and (3).

$$l_n = \frac{c}{4f_n\sqrt{\varepsilon_{re}}} \tag{1}$$

$$\varepsilon_{re} = \frac{\varepsilon_r + 1}{2} \tag{2}$$

$$l_t \approx l_n = Xn{+}Yn - t2 \tag{3}$$

ε_{re} — Relative dielectric constant of FR4,

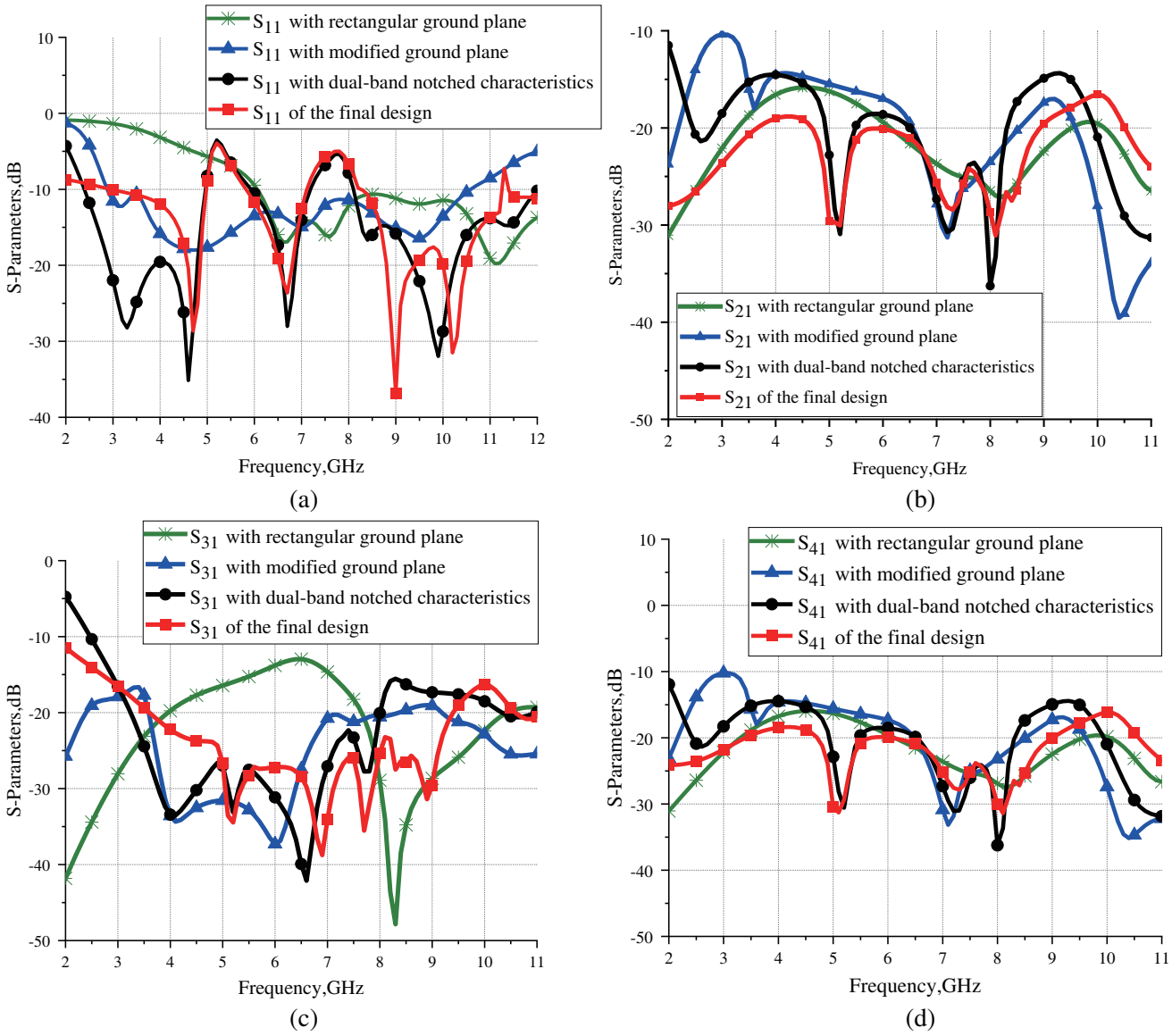

Figure 3. S-Parameters of the antenna: (a) S_{11}; (b) S_{21}; (c) S_{31}; (d) S_{41}.

f_n — The frequency of notch,
C – Specifies the speed of light in air,
l_n — The quarter wavelength of the notch frequency,
l_t — The actual length of each inverted L-shaped slit,
Xn, Yn, and $t2$ — The specific size of each inverted L-shaped slit in Figure 1(c).

In order to explain the principle of notch generation, the surface current distributions of the proposed MIMO antenna are simulated at the two notched frequencies of 5.20 GHz and 7.40 GHz. Figure 4 shows the results when Port 1 is excited, and Port 2 is connected to 50 ohm matching load. It can be seen that the surface currents are mainly concentrated in the long L-shaped slit and short L-shaped slit. For each slit, the currents on the two sides flow in opposite directions, which will be cancelled by each other. This is how a narrow band of suppression is processed to achieve a notch band. The length of the two inverted L-shaped slits is approximately equal to 1/4 of the wavelengths of 5.20 GHz and 7.40 GHz, respectively, which produces resonances at the corresponding frequency points.

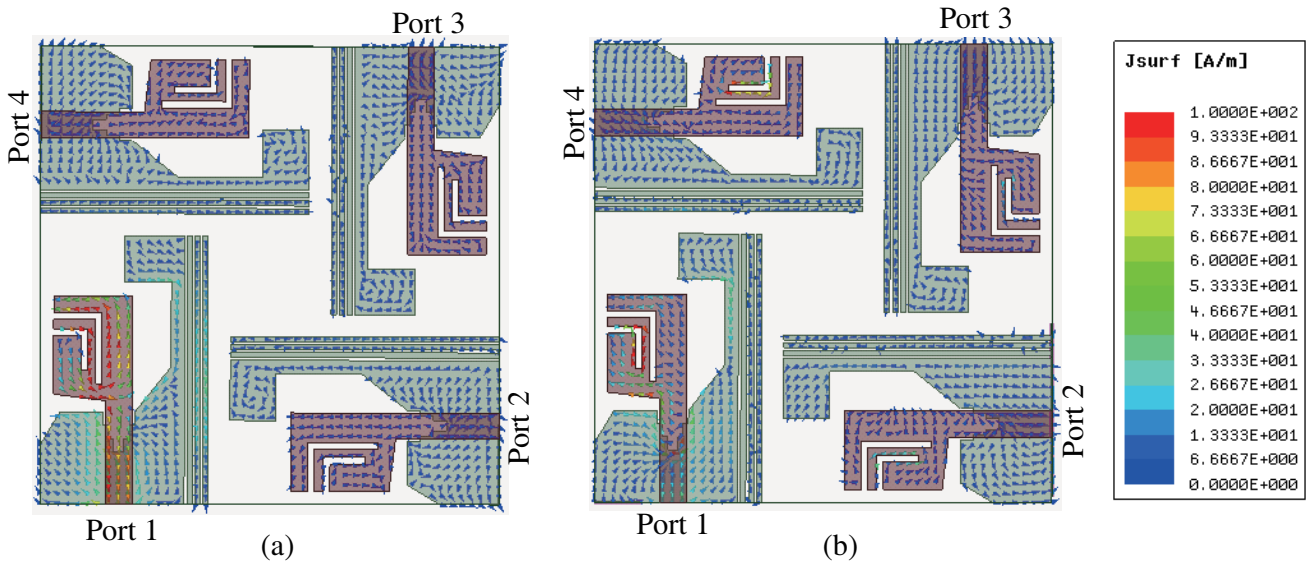

Figure 4. Surface current distributions of the MIMO antenna at double notched frequencies: (a) 5.20 GHz and (b) 7.40 GHz.

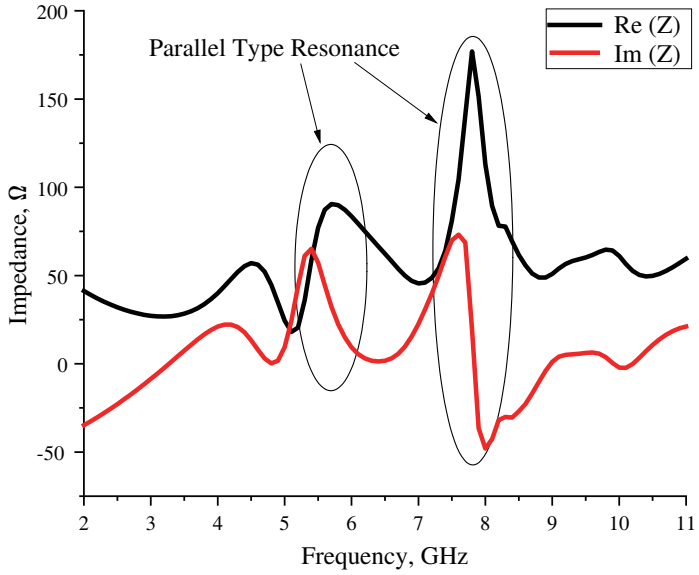

Figure 5. Characteristic impedance curve of the proposed UWB MIMO antenna.

Figure 5 shows the characteristic impedance curve of the proposed antenna. The real parts of the impedance curve at 5.2 GHz and 7.4 GHz are 21 Ω and 64 Ω, respectively. The imaginary parts of the impedance curve change from positive to negative, so both inverted L-shaped slits can be equivalent to parallel circuit models. The equivalent circuit of the notch bands with two parallel RLC resonators is shown in Figure 6. In Figure 6, the first resonator is designed to operate at 5.2 GHz and the second at 7.4 GHz. The corresponding Q_0 and lumped element values are then calculated at 5.20 GHz and 7.40 GHz and are listed in Table 2. The lumped elements calculation is carried out by Equations (4), (5), and (6),

$$Q_0 = \frac{f}{BW} \tag{4}$$

$$Q_0 = 2\pi f_0 RC \tag{5}$$

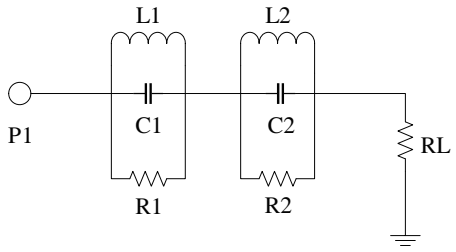

Figure 6. Equivalent lumped element model of the notch bands.

Table 2. Calculated values of the lumped elements.

Circuit	BW (MHz)	Q_0	R (Ω)	C (pF)	L (pH)
1	840	6.190	21	9.022	0.0104
2	1150	6.435	64	2.163	0.0214

$$f_0 = \frac{1}{2\pi\sqrt{LC}} \tag{6}$$

where f_0 is the resonant notched frequency, R the resistor, L the inductor, and C the capacitor of RLC circuit.

2.3. Decoupling Principle

Three equidistant rectangular decoupling slits are etched on the modified ground planes to reduce S_{21} values in Figure 3(b). Figure 7 shows the surface current distributions of the proposed MIMO antenna when Port 1 is excited at 4.0 GHz for example. The results show that the mutual couplings among the elements of the proposed antenna are much weaker than those of the antenna without the decoupling structure. As shown in Figure 3(b), the structure gets an S_{21} below -19 dB at lower frequencies than 8.93 GHz.

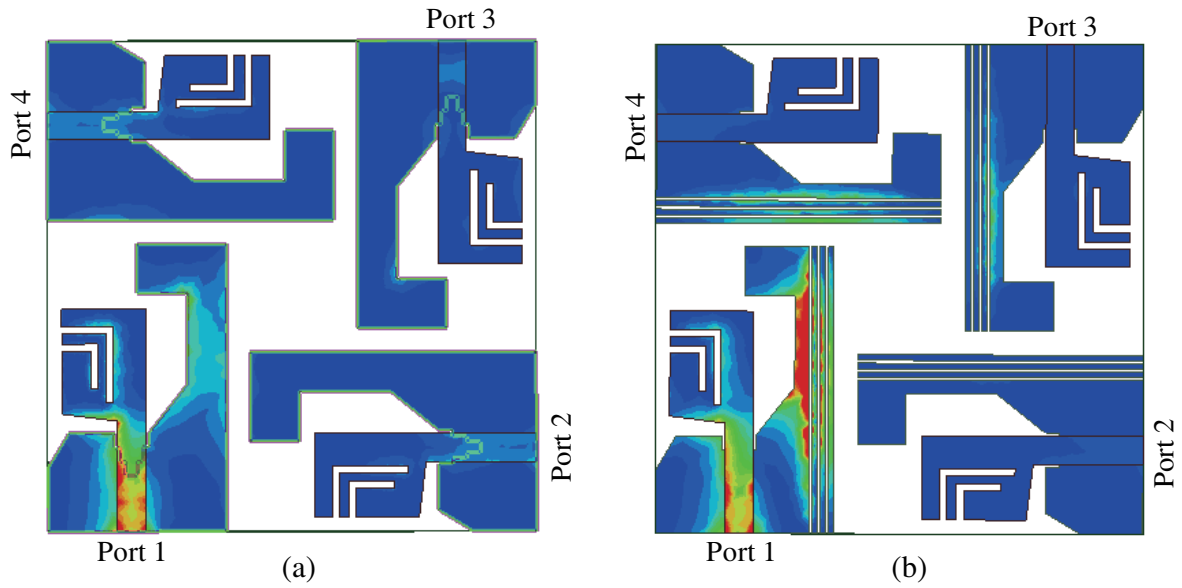

Figure 7. Current distributions of the MIMO antenna: (a) without decoupling slot and (b) with a decoupling.

3. RESULTS AND DISCUSSIONS

The proposed MIMO antenna was manufactured, and a physical image is shown in Figure 8. Its S-parameters were measured by a vector network analyzer, and the radiation patterns of the antenna were measured in a microwave anechoic chamber as well. Consider that the four radiation elements are identical, and Port 1 is taken as excitation for simplicity during measurement. The S parameters, radiation patterns at 4.0, 6.5, 8.0 GHz are measured and compared with simulation results in HFSS 15.0 as shown in Figure 9 and Figure 10. The gain, envelope correlation coefficient (ECC), diversity gain (DG), total active reflection coefficient (TARC), and channel capacity loss (CCL) over the entire band are compared in Figure 11–Figure 14, respectively. As can be seen:

(1) In Figure 9, the measured results of the antenna are in good agreement with the simulated ones. The measured bandwidth of S_{11} is 3.19 GHz–11.02 GHz, with two notches of 4.91 GHz–5.53 GHz and 7.14 GHz–8.23 GHz. The values of S_{21}, S_{31}, S_{41} are all less than −17 dB at the entire operating

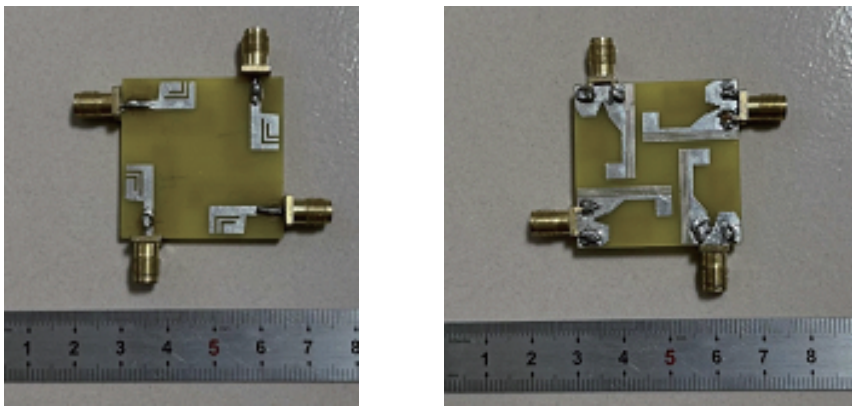

Figure 8. A physical image of the antenna: (a) top view and (b) bottom view.

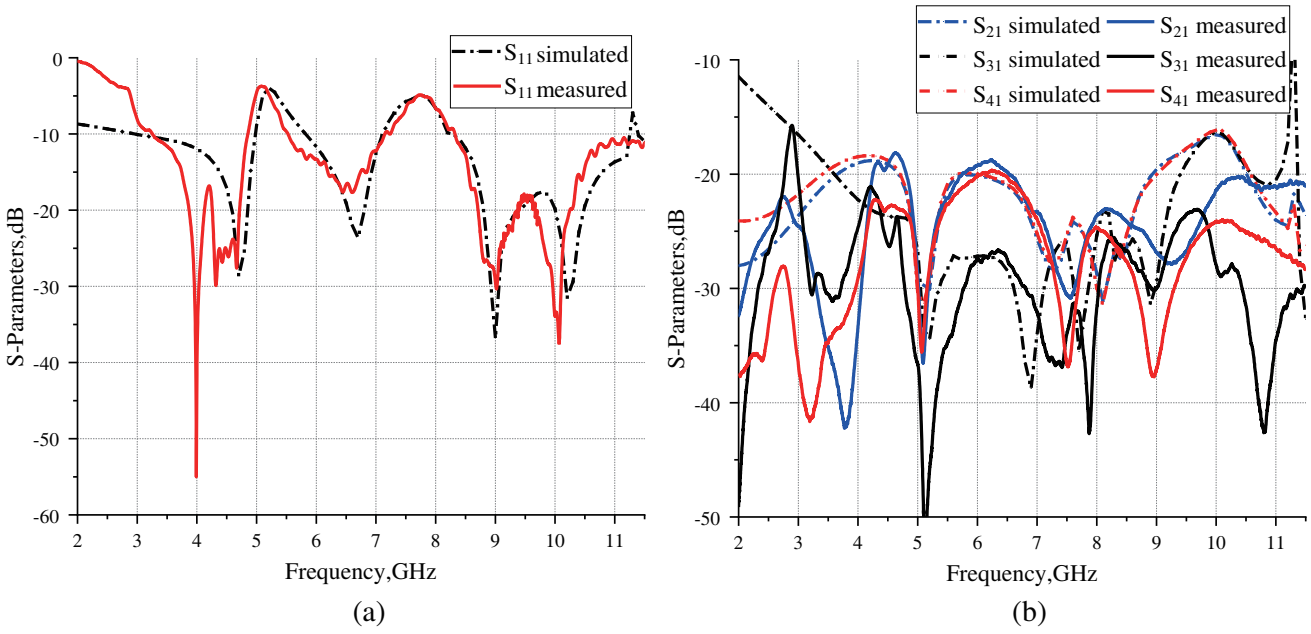

Figure 9. Simulated and measured S-Parameters of the proposed UWB MIMO antenna: (a) S_{11} and (b) S_{21}, S_{31}, and S_{41}.

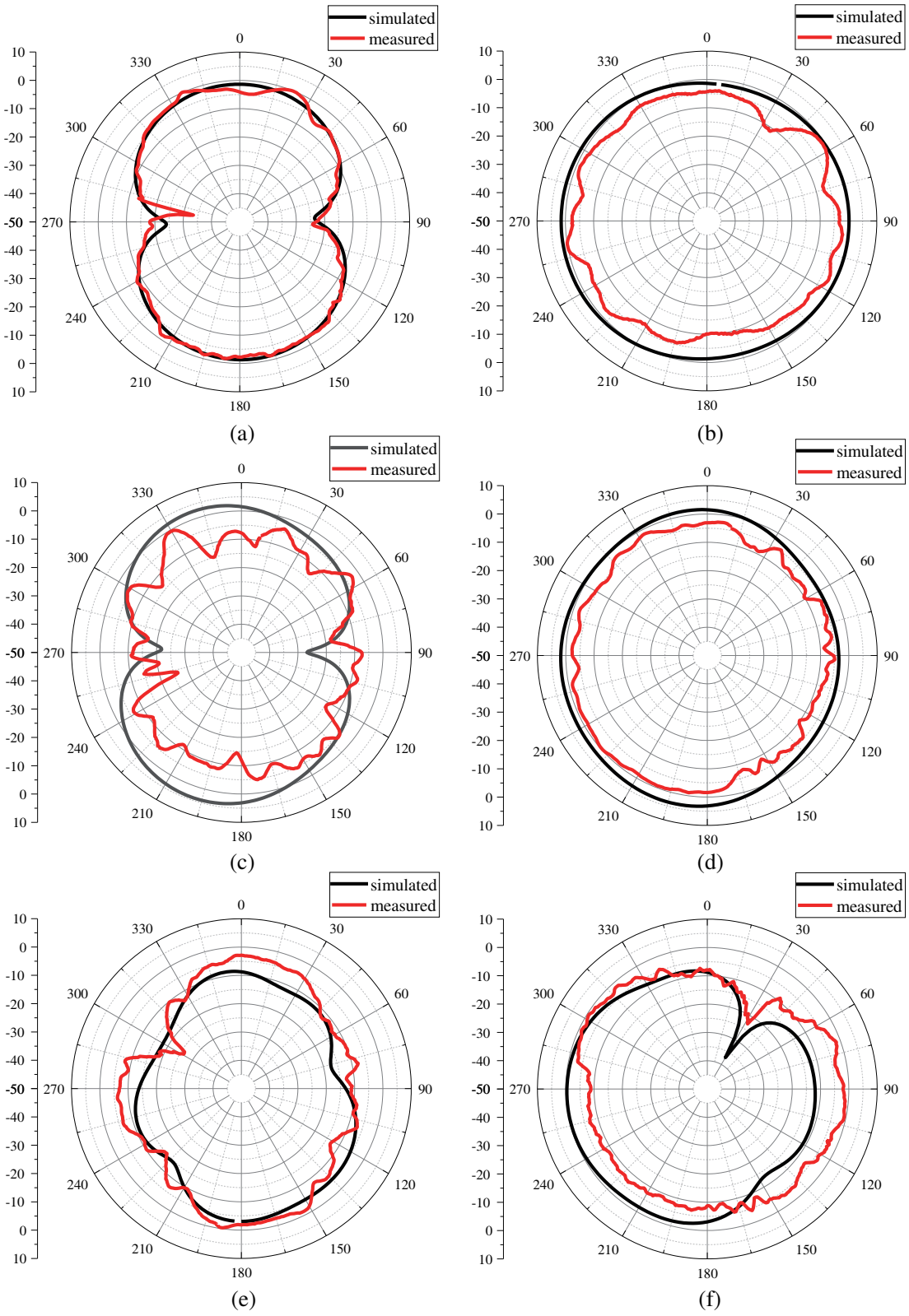

Figure 10. Radiation patterns at (a) 4.0 GHz (E-plane); (b) 4.0 GHz (H-plane); (c) 6.5 GHz (E-plane); (d) 6.5 GHz (H-plane); (e) 8.0 GHz (E-plane); (f) 8.0 GHz (H-plane).

frequency band, indicating that the antenna is of good isolation. The values of S_{21} and S_{41} are almost identical due to the symmetrical structure.

(2) Figure 10 shows that at the three sample frequencies, the radiation patterns in H-plane are nearly omnidirectional, while those in E-planes are bidirectional radiation model. Because of the symmetry of the antenna, the other ports exhibit similar radiation patterns.

(3) As for the antenna gain in Figure 11, it is ranged from -2.5 to 5 dBi as the frequency changes. The gain at the notch band of 5.20 GHz and 7.40 GHz drops significantly, indicating that the narrowband interference can be suppressed effectively. Besides, a peak value appears at 3.2 GHz. That is because the equidistant rectangular decoupling slits reduces the coupling at low frequency and generates a new resonant mode.

(4) In an isotropic channel condition, the envelope correlation coefficient (ECC) can be calculated

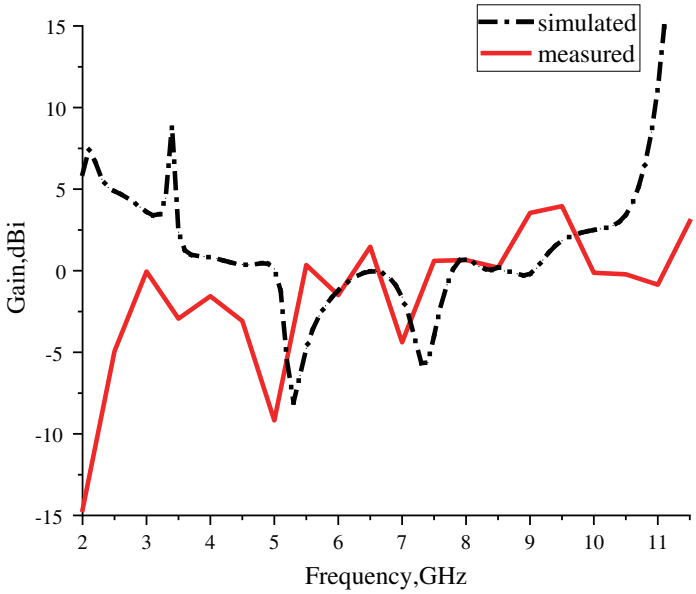

Figure 11. Simulated and measured gain over the entire band.

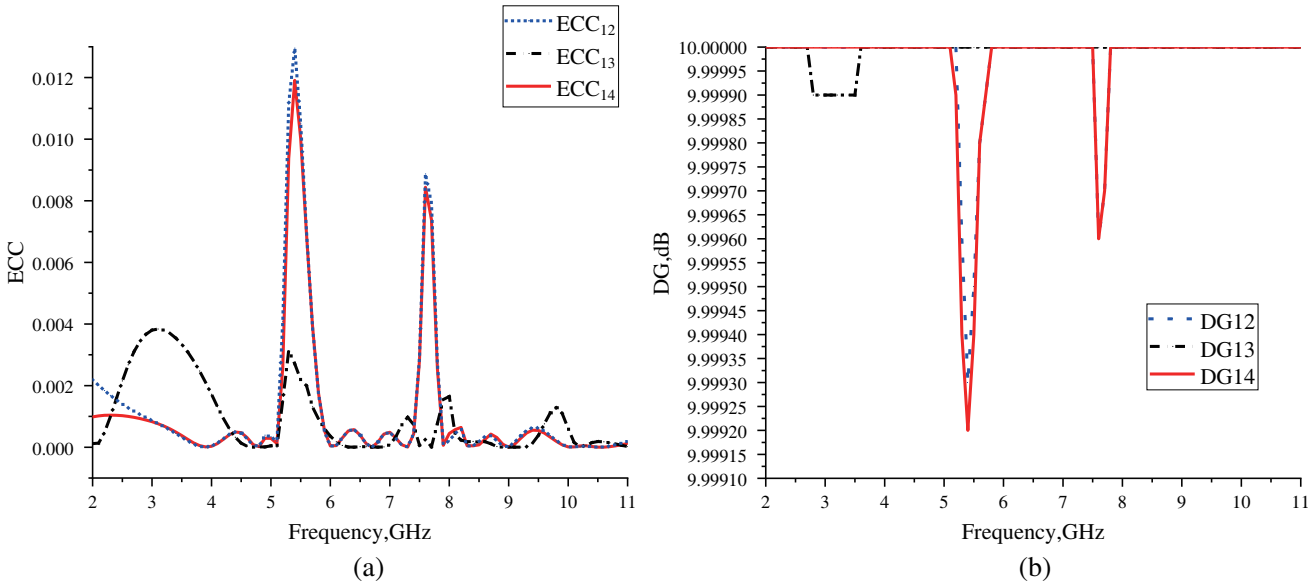

Figure 12. Diversity performance: (a) ECC and (b) DG.

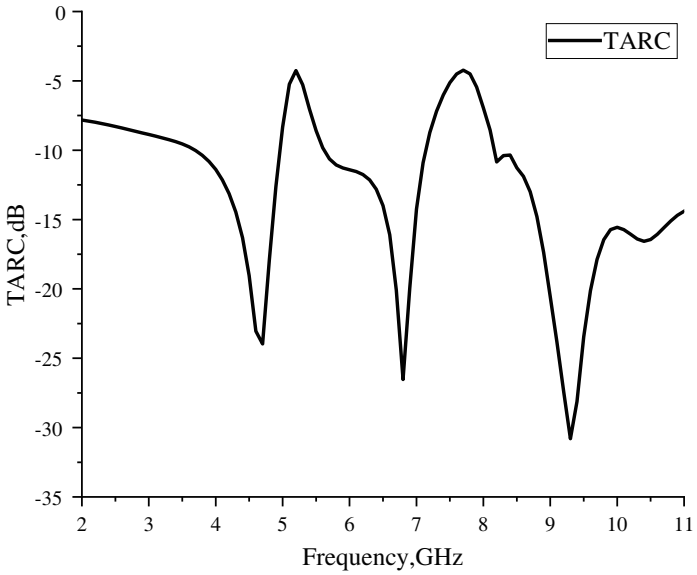

Figure 13. TARC of the proposed UWB MIMO antenna.

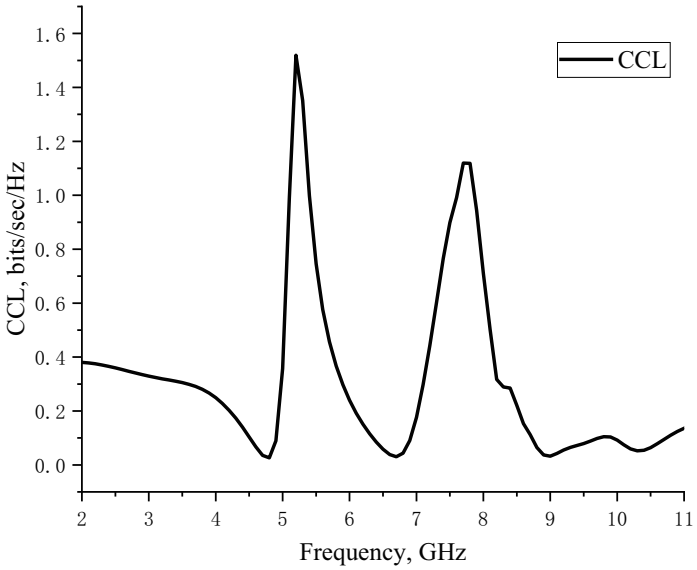

Figure 14. CCL of the proposed UWB MIMO antenna.

by Equation (7).

$$\rho_{eij} = \left| \frac{\left| \oint A_{ij}(\Omega) d\Omega \right|}{\sqrt{\oint A_{ii}(\Omega) d\Omega \oint A_{jj}(\Omega) d\Omega}} \right|^2 \tag{7}$$

The DG of proposed MIMO antenna is given by Equation (8),

$$\mathrm{DG} = 10\sqrt{1 - |\rho|^2} \tag{8}$$

where ρ is the complex cross correlation coefficient, and $|\rho|^2 \approx$ ECC. The simulated ECC values are below 0.004 (< 0.005) except the notch frequency bands in Figure 12(a). Diversity gain is greater than

9.9 dB across the whole impedance spectrum excluding dual notches in Figure 12(b). It exhibits that the suggested design has smaller ECC and superior DG, implying a good channel capacity.

(5) TARC defines MIMO antenna effective operating bandwidth with multiple ports. It is achieved from S-parameters (two port network) as given in Equation (9),

$$\Gamma_a^t = \sqrt{\frac{\left(\left(|S_{11} + S_{12}e^{j\theta}|^2\right) + \left(|S_{21} + S_{22}e^{j\theta}|^2\right)\right)}{2}} \tag{9}$$

where θ is the input feeding phase, and it ranges from 0 to π. Figure 13 illustrates TARC characteristics of the proposed quad element MIMO antenna for $\theta = 0°$. This parameter is less than -10 dB in the entire frequency range except the notch characteristics in 5.20 GHz and 7.40 GHz bands.

(6) The channel capacity loss is calculated numerically by Equation (10),

$$\text{CCL} = -\log_2 \det\left(\psi^R\right) \tag{10}$$

where

$$\psi^R = \begin{vmatrix} \rho_{11} & \rho_{12} & \rho_{13} & \rho_{14} \\ \rho_{21} & \rho_{22} & \rho_{23} & \rho_{24} \\ \rho_{31} & \rho_{32} & \rho_{33} & \rho_{34} \\ \rho_{41} & \rho_{42} & \rho_{43} & \rho_{44} \end{vmatrix} \tag{11}$$

$$\rho_{ii} = 1 - \sum_{n=1}^{4} |S_{in}|^2 \tag{12}$$

$$\rho_{ij} = -(S_{ii}^* S_{ij} + S_{ji}^* S_{ij}) \tag{13}$$

Usually, the CCL value is supposed to be less than 0.4 bits/sec/Hz for the entire working range. As shown in Figure 14, the CCL is good in most of the operating band, excluding the notched band at 5.20 GHz and 7.40 GHz in UWB range.

Finally, the proposed four-element MIMO antenna is compared with several previously reported MIMO antennas in terms of antenna size, bandwidth, isolation, and the number of notches. It is demonstrated in Table 3 that the proposed antenna has commensurate isolation performance but more compact structure and wider bandwidth in condition of two notches. And this good comprehensive performance enables it to be widely used in various UWB positioning systems.

Table 3. Comparison of various four-element MIMO antenna.

Ref. No	Antenna size (mm^3)	Bandwidth (GHz)	Mutual coupling (dB)	No. of Notches
[20]	$40 \times 40 \times 1.6$	3.1 GHz–10.6 GHz	> 19	1
[21]	$40 \times 40 \times 1.524$	3.0 GHz–13.5 GHz	> 15	0
[23]	$45 \times 45 \times 1.6$	2.2 GHz–6.28 GHz	> 14	0
[24]	$80 \times 80 \times 0.764$	3.6 GHz–10.6 GHz	> 20	0
[25]	$40 \times 40 \times 1.6$	3.1 GHz–11.0 GHz	> 20	0
[26]	$37 \times 46 \times 1.5$	2.5 GHz–12 GHz	> 20	2
[27]	$50 \times 35 \times 1.0$	3.0 GHz–11 GHz	> 25	0
[28]	$48 \times 48 \times 1.62$	4.5 GHz–10.6 GHz	> 20	0
[29]	$60 \times 60 \times 1.6$	3.0 GHz–16.2 GHz	> 17.5	0
Pro	$35 \times 35 \times 1.6$	2.96 GHz–11.25 GHz	> 17	2

4. CONCLUSION

In this paper, a miniaturized UWB MIMO antenna with dual-band notched characteristics is designed for a UWB indoor positioning system. Each of the four elements is composed of an irregular pentagon patch and an elaborately modified ground plane. The notch characteristic is obtained by etching two inverted L-shaped slits on each radiating patch. Three equidistant rectangular decoupling slits are etched on the modified ground to achieve high isolation. The simulated and measured results show that the bandwidth of the antenna covers 3.10 GHz–10.60 GHz with two notches in WLAN and X-band and isolation less than −17 dB. In the entire operating frequency range, the antenna patterns have good isotropic radiation characteristics; the ECC of the antenna is less than 0.005; DG values are very near 10; effective operating band obtained from TARC characteristics closely resembles the operating band obtained from S-parameter characteristics; CCL values are less than 0.4 bits/sec/Hz. Above all, the proposed antenna has good comprehensive performance and meets the design requirements of an UWB indoor positioning system.

ACKNOWLEDGMENT

This work is supported in part by the NSF Foundation of China (No. 62276162) and Fundamental Research Program of Shanxi Province (202103021223029).

REFERENCES

1. Gigl, T., G. J. M. Janssen, V. Dizdarevic, et al., "Analysis of a UWB indoor positioning system based on received signal strength," *Workshop on Positioning IEEE*, 97–101, Hannover, 2007.
2. Mahato, S., S. Modak, T. Khan, et al., "Triple notched-band slots-loaded arrow-head shaped UWB monopole antenna," *Advanced Communication Technologies and Signal Processing (ACTS)*, 1–4, Silchar, 2020.
3. Li, W. A., Z. H. Tu, Q. X. Chu, et al., "Differential stepped-slot UWB antenna with common-mode suppression and dual sharp-selectivity notched bands," *IEEE Antennas and Wireless Propagation Letters*, Vol. 15, 1120–1123, 2016.
4. Kang, L., H. Li, X. Wang, et al., "Compact offset microstrip-fed MIMO antenna for band-notched UWB applications," *IEEE Antennas and Wireless Propagation Letters*, Vol. 14, 1754–1757, 2015.
5. Rahman, M. U., A. Haider, and M. Naghshvarianjahromi, "A systematic methodology for the time-domain ringing reduction in UWB band-notched antennas," *IEEE Antennas and Wireless Propagation Letters*, Vol. 19, No. 3, 482–486, 2020.
6. Liu, Y. Y. and Z. H. Tu, "Compact differential band-notched stepped-slot UWB-MIMO antenna with common-mode suppression," *IEEE Antennas and Wireless Propagation Letters*, Vol. 16, 593–596, 2017.
7. Abbas, A., N. Hussain, J. Lee, et al., "Triple rectangular notch UWB antenna using EBG and SRR," *IEEE Access*, Vol. 9, No. 99, 2508–2515, 2020.
8. Sanyal, R., A. Patra, P. P. Sarkar, et al., "Compact UWB monopole antenna with 3.5/ 5.5 GHz enhanced dual band rejection characteristics," *Microwave and Optical Technology Letters*, Vol. 57, No. 11, 2693–2699, 2015.
9. Jafri, S. I., R. Saleem, and K. Khokhar, "CPW-fed UWB antenna with tri-band frequency notch functionality," *Applied Computational Electromagnetics Society Journal*, Vol. 34, No. 9, 1274–1279, 2019.
10. Huang, H., Y. Liu, S. Zhang, et al., "Uniplanar differentially driven ultrawideband polarization diversity antenna with band-notched characteristics," *IEEE Antennas and Wireless Propagation Letters*, Vol. 14, No. 3, 563–566, 2015.
11. Tang, Z., X. Wu, J. Zhan, et al., "Compact UWB-MIMO antenna with high isolation and triple band-notched characteristics," *IEEE Access*, Vol. 7, No. 62, 19856–19865, 2019.

12. Raheja, D. K., S. Kumar, and B. K. Kanaujia, "Compact quasi-elliptical-self-complementary four-port super-wideband MIMO antenna with dual band elimination characteristics," *AEU — International Journal of Electronics and Communications*, Vol. 114, 153001, 2020.
13. Tan, X., W. Wang, Y. Wu, et al., "Enhancing isolation in dual-band meander-line multiple antenna by employing split EBG structure," *IEEE Transactions on Antennas and Propagation*, Vol. 67, No. 4, 2769–2774, 2019.
14. Chaabane, A. and F. Djahli, "A compact planar UWB antenna with triple controllable band-notched characteristics," *International Journal of Antennas and Propagation*, Vol. 2014, 1–10, 2015.
15. Sultan, K. S., O. Dardeer, and H. A. Mohamed, "Design of compact dual notched self-complementary UWB antenna," *Open Journal of Antennas & Propagation*, Vol. 5, No. 3, 99–109, 2017.
16. Xu, J. M., C. Z. Du, G. Y. Jin, et al., "A coplanar feed quad-band notched UWB antenna," *International Workshop on Electromagnetics: Applications and Student Innovation Competition (iWEM)*, 1–2, Qingdao, 2019.
17. Li, Z., C. Yin, and X. Zhu, "Compact UWB MIMO vivaldi antenna with dual band-notched characteristics," *IEEE Access*, Vol. 7, No99, 38696–38701, 2019.
18. Elkazmi, E., C. H. See, N. A. Jan, et al., "Design of a wideband printed MIMO monopole antenna using neutralisation lines technique," *Asia-Pacific Microwave Conference*, 983–985, Sendai, 2014.
19. Raheja, D. K., B. K. Kanaujia, S. Kumar, "Compact four-port MIMO antenna on slotted-edge substrate with dual-band rejection characteristics," *International Journal of RF and Microwave Computer-Aided Engineering*, Vol. 29, No. 7, 1–10, 2019.
20. Selvan, K., R. Sampath, and A. A. Arulraj, "Isolation improvement of UWB MIMO antenna utilizing molecule fractal structure," *Electronics Letters*, Vol. 10, No. 55, 576–579, 2019.
21. Khan, A. A., S. A. Naqvi, M. S. Khan, and B. Ijaz, "Quad port miniaturized MIMO antenna for UWB 11 GHz and 13 GHz frequency bands," *AEU — International Journal of Electronics and Communications*, Vol. 131, 153618, 2021.
22. Kamel, S. S. and H. H. Abdullah, "Planar UWB MIMO-diversity antenna with dual notch characteristics," *Progress In Electromagnetics Research C*, Vol. 93, 119–129, 2019.
23. Tiwaria, R. N., P. Singh, B. K. Kanaujia, and K. Srivastava, "Neutralization technique based two and four port high isolation MIMO antennas for UWB communication," *AEU-International Journal of Electronics and Communications*, Vol. 110, Article 152828, July 2019.
24. Naktong, W. and A. Ruengwaree, "Four-port rectangular monopole antenna for UWB-MIMO applications," *Progress In Electromagnetics Research B*, Vol. 87, 19–38, 2020.
25. Deepika, S., et al., "Compact planar 2×2 and 4×4 UWB MIMO antenna arrays for portable wireless devices," *Microwave and Optical Technology Letters*, Vol. 60, No. 1, 86–92, 2017.
26. Ali, W. and A. A. Ibrahim, "A compact double-sided MIMO antenna with an improved isolation for UWB applications," *AEU — International Journal of Electronics and Communications*, Vol. 82 7–13, 2017.
27. Wang, L., Z. Du, H. Yang, et al., "Compact UWB MIMO antenna with high isolation using fence-type decoupling structure," *IEEE Antennas and Wireless Propagation Letters*, Vol. 18, No. 8, 1641–1645, 2019.
28. Alfakhri, A., M. A. Ashraf, A. Alasaad, et al., "A compact size ultra wideband MIMO antenna with simple decoupling structure," *International Symposium on Antenna Technology & Applied Electromagnetic*, 1–2, Montreal, QC, 2016.
29. Wu, W., B. Yuan, and A. Wu, "A quad-element UWB-MIMO antenna with band-notch and reduced mutual coupling based on EBG structures," *International Journal of Antennas and Propagation*, Vol. 25, No. 2, 1–10, 2018.